Dist: A

AD-A284 113

PAGE

Form Approved
OMB No. 0704-0188

1. AGENCY USE ONLY (Leave blank)	2. REPORT DATE	3. REPORT TYPE AND DATES COVERED
	July 15, 1994	Reprints

4. TITLE AND SUBTITLE
Classical Intramolecular Energy-Transfer Rates Using Fourier Transform Methods: Four-Atom Systems

5. FUNDING NUMBERS
61102F 2303 FS

6. AUTHOR(S)
Xiao Yan Chang, Karen L. Bintz, Donald L. Thompson, and Lionel M. Raff

7. PERFORMING ORGANIZATION NAME(S) AND ADDRESS(ES)
Oklahoma State University
210 Life Sciences East
Stillwater, OK 74078-0266

8. PERFORMING ORGANIZATION REPORT NUMBER
1-5-19592

AFOSR-TR- 94 0528

9. SPONSORING/MONITORING AGENCY NAME(S) AND ADDRESS(ES)
AFOSR/NC
Building 410, Bolling AFB DC
20332-6448

10. SPONSORING/MONITORING AGENCY REPORT NUMBER
F49620-92-J-0011

11. SUPPLEMENTARY NOTES
Published in Journal of Physical Chemistry, 1994, 98, 6317.

12a. DISTRIBUTION/AVAILABILITY STATEMENT
APPROVED FOR PUBLIC RELEASE; DISTRIBUTION IS UNLIMITED.

A 8pg

12b. DISTRIBUTION CODE

94-29008

13. ABSTRACT (Maximum 200 words)

A previously reported [*J. Chem. Phys.* **1991**, *95*, 106; *Chem. Phys. Lett.* **1993**, *206*, 137] Fourier transform method for computation of classical intramolecular mode-to-mode energy-transfer rate coefficients is extended to four-atom molecules. HONO and C_2H_2 are used as test cases. The method involves the Fourier transform of the time variation of a local-mode bond energy for an ensemble of trajectories. A two-mode, collinear model is employed to demonstrate that the transform is expected to contain a series of spectral bands at frequencies corresponding to the mode-to-mode energy-transfer rates. Heavy-atom blocking and constrained motion methods are employed to determine the individual band assignments. The results for both HONO and C_2H_2 are in good accord with the total relaxation rate extracted from decay plots of the local-mode energy.

14. SUBJECT TERMS	15. NUMBER OF PAGES
Intramolecular Energy Transfer	7 per reprint
	16. PRICE CODE

17. SECURITY CLASSIFICATION OF REPORT	18. SECURITY CLASSIFICATION OF THIS PAGE	19. SECURITY CLASSIFICATION OF ABSTRACT	20. LIMITATION OF ABSTRACT
UNCLASSIFIED	UNCLASSIFIED	UNCLASSIFIED	UL

25 AUG 1994

Reprinted from The Journal of Physical Chemistry, 1994, 98.

Classical Intramolecular Energy-Transfer Rates Using Fourier Transform Methods: Four-Atom Systems

Xiao Yan Chang, Karen L. Bintz, Donald L. Thompson, and Lionel M. Raff*

Department of Chemistry, Oklahoma State University, Stillwater, Oklahoma 74078

*Received: February 3, 1994; In Final Form: April 11, 1994**

A previously reported [*J. Chem. Phys.* **1991**, *95*, 106; *Chem. Phys. Lett.* **1993**, *206*, 137] Fourier transform method for computation of classical intramolecular mode-to-mode energy-transfer rate coefficients is extended to four-atom molecules. HONO and C_2H_2 are used as test cases. The method involves the Fourier transform of the time variation of a local-mode bond energy for an ensemble of trajectories. A two-mode, collinear model is employed to demonstrate that the transform is expected to contain a series of spectral bands at frequencies corresponding to the mode-to-mode energy-transfer rates. Heavy-atom blocking and constrained motion methods are employed to determine the individual band assignments. The results for both HONO and C_2H_2 are in good accord with the total relaxation rate extracted from decay plots of the local-mode energy.

I. Introduction

We have previously described[1,2] a Fourier transform (FT) method for extracting classical intramolecular vibrational energy-transfer rates (FTIVR). The FTIVR method involves the computation of the time dependence of some local-mode bond energy, $E_b(t)$, in the molecule from the ensemble average of a set of classical trajectories computed using standard techniques.[3] This bond energy exhibits characteristic fluctuations due to energy-transfer processes between the various modes in the molecule. Consequently, the FT of $E_b(t)$ should, in principle, yield a spectrum that contains bands at frequencies corresponding to the mode-to-mode rate coefficients.

In previous applications, we have investigated mode-to-mode energy-transfer rates in the ethynyl (C_2H) radical[1] and disilane.[2] In the case of C_2H, three distinct bands appear in the FTIVR spectrum in the frequency range 0.01–0.18 ps^{-1}. The frequencies of these bands are interpreted to represent the average mode-to-mode energy-transfer rates for IVR *via* the stretch/stretch and two stretch/bend pathways. It is shown that these mode-to-mode rates are in good accord with the total relaxation rate extracted from decay plots of the C–H local-mode energy. We have also applied the FTIVR method to intramolecular energy transfer in disilane.[2] The result is a series of broad peaks spanning the range 0.01–0.3 ps^{-1} with a global maximum at 0.07 ps^{-1}. This suggests that the IVR rates in disilane are described by a set of coefficients whose values lie in the range 0.01–0.3 ps^{-1} with a most probable value of 0.07 ps^{-1}. This interpretation was shown to be consistent with the total relaxation rate of the Si–H local mode extracted by least-squares fitting of the decay curves obtained from the trajectory calculations. Unfortunately, the resolution of the spectral bands was insufficient to permit the individual coefficients to be determined. This difficulty arises, in part, because of the large number (153) of mode-to-mode coefficients involved.

In the present paper, we first explore the FTIVR method in a simple model system which permits a more detailed investigation than is possible in more complex molecular systems. We then show that the FTIVR method can be effectively extended to four-atom molecules. HONO and acetylene are chosen as test cases. This choice is dictated by the availability of accurate intramolecular potentials and by the fact that C_2H_2 and HONO represent both linear and nonlinear cases.

II. Application to a Simple Model System

Consider an ensemble of N local vibrational modes. If the coupling terms between these modes are zero, each will correspond to a good action variable, and the corresponding mode energies will be constants of the motion. A Fourier transform of the mode energies would therefore exhibit only a single component at zero frequency. If, however, the coupling terms are nonzero, intramolecular energy flow between the modes will be observed and the mode energies will vary with time. The basic premise of the FTIVR method is that since the fluctuations of the mode energies are produced by mode-to-mode energy transfer, the corresponding rates for these underlying processes must be embedded in the time-varying behavior of the local-mode energies.

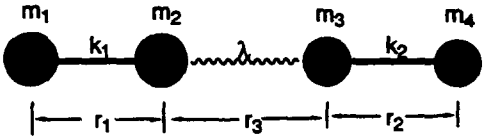

Figure 1. Definition of variables in the two-mode, collinear model.

Consider a simple collinear system consisting of two harmonic oscillators with a quadratic coupling potential. A diagram of this system is shown in Figure 1. We take the system Hamiltonian to be

$$H = [P_1^2/2m_1 + P_2^2/2m_2 + k_1(r_1 - R_{e1})^2] + [P_3^2/2m_3 + P_4^2/2m_4 + k_2(r_2 - R_{e2})^2] + \lambda(r_3 - R_{e3})^2 \quad (1)$$

where the m_i (i = 1, 2, 3, 4) are the atomic masses, P_i are the momenta, and the r_i are interatomic distances as defined in Figure 1. The local mode energies are

$$E_1 = [P_1^2/2m_1 + P_2^2/2m_2 + k_1(r_1 - R_{e1})^2] \quad (2)$$

and

$$E_2 = [P_3^2/2m_3 + P_4^2/2m_4 + k_2(r_2 - R_{e2})^2] \quad (3)$$

If the coupling constant λ is zero, E_1 and E_2 will be constants of the motion. For $\lambda \neq 0$, the modes will be coupled and energy transfer will occur between them.

We have investigated the nature of the energy transfer for the above system for a total energy of 0.50 eV initially contained in mode 1. The system parameters are given in Table 1. Figure 2, a and b, shows the time variation of E_1 for λ equal to 0.45 and 0.60 eV/Å^2, respectively. Several qualitative features of the energy transfer between modes 1 and 2 are immediately evident. First, the mode-to-mode energy transfer produces characteristic oscillations in the local-mode energy. Second, the oscillations resulting from energy transfer between modes 1 and 2 have higher

* Abstract published in *Advance ACS Abstracts*, June 1, 1994.

0022-3654/94/2098-6317$04.50/0

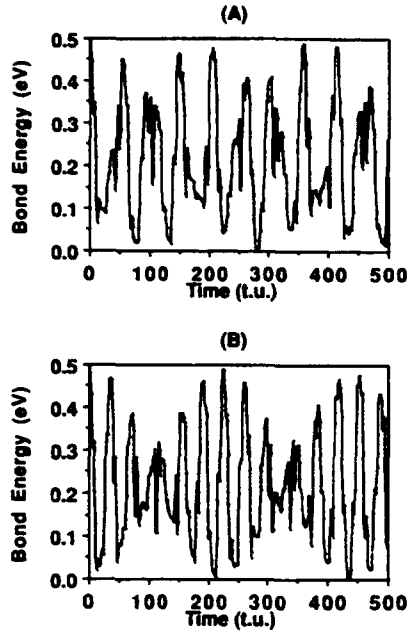

Figure 2. Energy in local mode 1 as a function of time: (A) $\lambda = 0.45$ eV/Å^2, (B) $\lambda = 0.60$ eV/Å^2. Time is given in units tu, where 1 tu = 1.019×10^{-14} s.

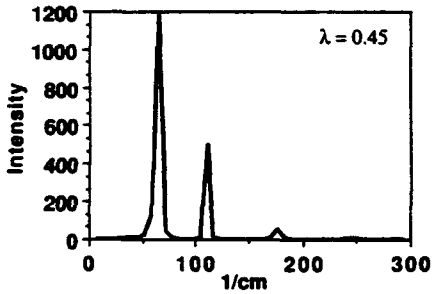

Figure 3. Fourier transform of the local mode bond energy $E_1(t)$ given in Figure 2A.

TABLE 1: Parameters of the Two-Mode, Collinear IVR Model

k_1	1.00 eV/Å^2	R_{e2}	1.00 Å	m_2	10.00 amu
k_2	1.00 eV/Å^2	R_{e3}	1.50 Å	m_3	10.00 amu
R_{e1}	1.00 Å	m_1	10.00 amu	m_4	10.00 amu

frequency oscillations superimposed upon them. Third, the mode-to-mode energy transfer rate increases as the coupling constant λ increases.

Figure 3 shows the Fourier transform of E_1 given in Figure 2a for $\lambda = 0.45$ eV/Å^2. The FT spectrum shows three features. The most important of these is a band at 65.5 cm^{-1}, which corresponds to a frequency of 2.0×10^{12} s^{-1} and a period of 5.0×10^{-13} s. In the molecular time units being used in Figure 2a,b, this corresponds to a period of 49.07 tu (1 tu = 1.019×10^{-14} s). An inspection of Figure 2a shows that after 500 tu the local-mode energy E_1 has executed about 9.5 complete oscillations. Obviously, the major FT spectral band at 65.5 cm^{-1} corresponds to the frequency at which energy is transferred between the modes. A similar Fourier transform of Figure 2b yields a three-band spectrum with the major peak at 85.2 cm^{-1}, which corresponds to the mode-to-mode energy-transfer rate seen with $\lambda = 0.60$ eV/Å^2.

The small peak in the FT spectrum at 176.9 cm^{-1} is the result of the higher frequency component seen in Figure 2a. These oscillations reflect energy transfer in and out of the coupling term in eq 1 rather than actual transfer to mode 2. This is easily seen from the transform of the coupling term alone. This is shown in Figure 4 for the case $\lambda = 0.45$ eV/Å^2. The only prominent feature is a band at 176.9 cm^{-1}. Finally, the remaining band in

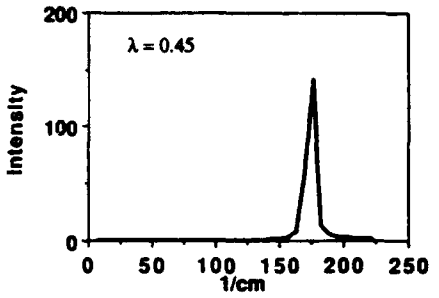

Figure 4. Fourier transfer of the time variation of the coupling term with $\lambda = 0.45$ eV/Å^2.

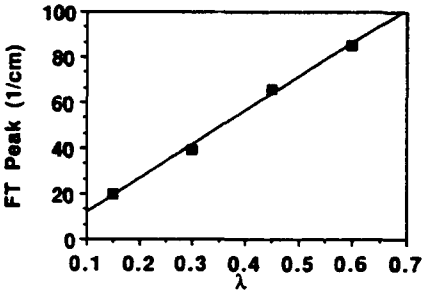

Figure 5. Dependence of the frequency of the energy-transfer FT band on the coupling constant, λ.

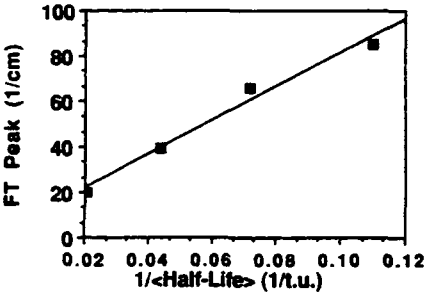

Figure 6. Dependence of the frequency of the energy-transfer FT band on the inverse of the average half-life, $\langle t_{1/2} \rangle$, computed for different values of λ.

the FT spectrum of $E_1(t)$ is a peak at 111.4 cm^{-1}. This frequency is the difference between the energy-transfer band at 65.5 cm^{-1} and the coupling term band at 176.9 cm^{-1}. The peak at 111.4 cm^{-1} may therefore be identified as the combination band (ν_{176}–ν_{65}).

Since the frequency of the energy-transfer band in Figure 3 measures the rate of mode-to-mode energy transfer, we would expect it correlate directly with the magnitude of the coupling term connecting the two modes. Figure 5 shows the calculated frequency of the energy-transfer band as a function of the coupling constant λ. The direct correlation is obvious.

The data shown in Figure 2a,b make it clear that energy transfer in the model system cannot be described by a first-order rate law. It is therefore not possible to define a rate coefficient in the usual manner as the negative slope of a logarithmic decay curve. We can, however, obtain a second measure of the transfer rate by computation of an average half-life, $\langle t_{1/2} \rangle$. This is most conveniently done by averaging the results of M trajectories differing only in the initial phase of local mode 1 and computing the times required for the peak energies in mode 1 to decrease to half of their initial values. $\langle t_{1/2} \rangle$ is defined as the ensemble average of these values. Since $\langle t_{1/2} \rangle^{-1}$ is a measure of the energy-transfer rate, we would expect a direct correlation to exist between the values of $\langle t_{1/2} \rangle^{-1}$ obtained for different values of λ and the frequencies of the energy-transfer band in the FT spectrum of E_1. Figure 6 shows that the correlation between these quantities is excellent.

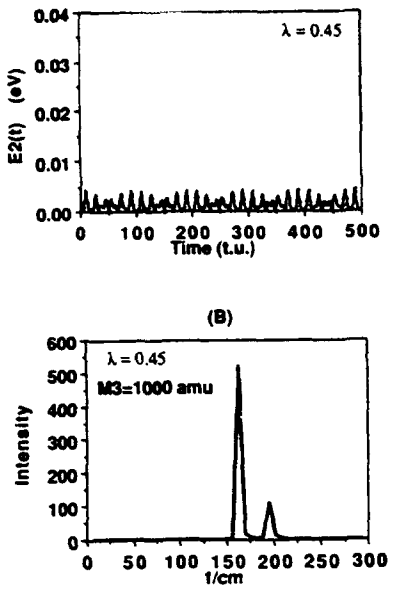

Figure 7. Heavy-atom blocking effects. (A) Time variation of the energy in local mode 2 for $E = 0.50$ eV initially partitioned into mode 1 with $M_3 = 1000$ amu and $\lambda = 0.45$ eV/Å^2. Other parameters are as given in Table 1. (B) Fourier transform of local mode energy 1, $E_1(t)$, for the case described in Figure 7A.

If the mode 1 → mode 2 path is effectively blocked by assigning a very large mass to atom 3, we expect the energy-transfer rate to approach zero and for the FT band corresponding to this mode-to-mode rate to decrease significantly in intensity or to vanish entirely. Figure 7a shows $E_2(t)$ for the case $M_3 = 1000$ amu and $\lambda = 0.45$ eV/Å^2, with the remaining parameters being those given in Table 1. Obviously, the energy-transfer path is essentially blocked. No more than 10% of the total energy initially present in mode 1 ever finds its way into mode 2. Figure 7b shows the FT spectrum of $E_1(t)$ for this case. As can be seen, the energy-transfer band at 65.5 cm^{-1} has vanished along with the combination band at 111.4 cm^{-1}. Only the mode coupling band remains. This peak is slightly red-shifted to 163.8 cm^{-1} due to the effect of the heavy-atom mass.

The above analysis shows that the frequency of the energy-transfer band in the FT spectrum correlates directly with the magnitude of the mode-to-mode coupling term and with other measures of the transfer rate such as $\langle t_{1/2} \rangle^{-1}$. Examination of the time dependence of E_1 shown in Figure 2a demonstrates that the FT band frequency corresponds exactly to the energy-transfer rate. Elimination of energy transfer by heavy-atom blocking eliminates the energy-transfer band entirely. It is therefore appropriate to take the frequency of the FT energy-transfer band to be the characteristic mode-to-mode transfer rate.

We now consider how the existence of many vibrational modes in a three-dimensional molecular system would be expected to alter the results obtained for the two-mode, collinear model shown in Figure 1. First, there will be many additional energy-transfer pathways, each with its own characteristic frequency and coupling terms. We will therefore expect the FT spectrum to contain many bands. Some of these will correspond to mode-to-mode energy-transfer rates; others will be associated with rates of energy transfer to and from the coupling terms. In addition, we expect to find combination bands and perhaps some overtone bands. Identification of these bands will therefore pose a significant problem which is analogous to the experimental problem of assigning IR absorption bands to particular vibrational modes in the molecule.

Because of the presence of many transfer pathways, we expect entropy effects to significantly reduce the amplitude of the oscillations in the local-mode energies. However, we still expect them to be present. If there are enough coupled modes, the oscillation amplitudes may be reduced to the point that the envelope function begins to resemble an exponential decay which will permit us to extract a total energy-transfer coefficient out of mode i, K^i_T, which will be the sum of all of the mode-to-mode rates, $k_{i\to j}$,

$$K^i_T = \sum_j k_{i\to j} \tag{4}$$

In such a case, we expect the sum of the frequencies of the FT energy-transfer bands to correlate directly with K^i_T determined from the slope of the logarithmic decay curve. We have previously shown that this is the case for C_2H and disilane. In the present paper, we also show that it is true for HONO.

Finally, since there will be many and varied coupling terms present in the complex potential representing a real molecule with numerous vibrational modes, we expect the time variation of the local-mode energy to exhibit many high-frequency oscillations superimposed upon lower frequency oscillations which correspond to the energy-transfer bands whose amplitudes will be a decreasing function of time.

The calculation of an FTIVR spectrum has the dual advantages that it is very easy to compute and it contains all of the mode-to-mode rates. The two major difficulties associated with the method involve band resolution and assignment. If there are many mode-to-mode bands, it may be impossible to resolve them. This is analogous to the problem of resolving the rotational bands in a large molecule. The first difficulty may be minimized to some extent by extending the computation time for the trajectories which will increase the FT resolution. The second problem may be attacked using heavy-atom blocking and constrained motion methods. These methods are described in more detail in the following section.

III. Potential Energy Surfaces and Numerical Procedures

A. HONO. The potential energy surface used in the calculation is that employed in our previous energy-transfer studies.[4] Bond stretching potentials are represented by a summation of Morse potentials,

$$V_s = \sum_i D_{ei}\{(1.0 - \exp[-\alpha_i(R_i - R_{ei})])^2\} \tag{5}$$

Quadratic functions are used for the bending motions

$$V_b = \sum_i k_i(\theta_i - \theta_{ei})^2 \tag{6}$$

where the summation runs over all bending motions of the molecule. The torsional potential is given by

$$V_t = \sum_i a_i \cos(i\varphi) \tag{7}$$

where the R_i are bond lengths, θ_i are bending angles, and φ is the dihedral angle.

B. Acetylene. The analytical potential energy surface developed by White and Schatz[5] is employed for acetylene. This surface is based on fits to *ab initio* calculations of the molecular force field, experimentally derived energies of formation, and the isomerization barrier. The fitting procedure used for C_2H combines a LEPS potential with a three-body Sorbie–Murrell function[6] to fit the C_2H force field, the isomerization barrier, and the C_2H dissociation energies. For C_2H_2, two C_2H fragment potentials are combined with an empirical methylene potential and a four-body Sorbie–Murrell function[6] to fit the acetylene force field, the vinylidene minimum energy, and other information.

TABLE 2: C_2H_2 and HONO Normal-Mode Frequencies

molecule	mode no.	mode description	freq (cm^{-1})
C_2H_2[a]	1	C–H stretch	3400
	2	C–H stretch	3314
	3	C–C stretch	2022
	4–5	HCCH bend[b]	797
	6–7	HCCH bend[b]	569
HONO	1	O–H stretch	3438
	2	N=O stretch	1640
	3	O–N stretch	908
	4	HON bend	1306
	5	ONO bend	540
	7	torsion	649

[a] Computed on the White–Schatz potential surface, ref 5. [b] Doubly degenerate vibrational mode.

The fundamental vibrational frequencies for all of the HONO and acetylene normal modes computed using the above potentials are summarized in Table 2.

C. Numerical Procedures. The local bond mode energy is defined as

$$E_b(t) = (P_b(t)^2/2\mu_b) + V_b[r_b(t)] \quad (8)$$

where the reduced mass μ_b, momentum $P_b(t)$, and bond length $r_b(t)$ are those appropriate to the bond in question. The bond potential, $V_b[r_b(t)]$, is taken to be a Morse function with parameters chosen so that it corresponds closely to the bond potential on the full global surface.

Hamilton's equations of motion are integrated using a fourth-order Runge–Kutta integrator. The acetylene intramolecular dynamics are computed for a time period 196.6 ps using a fixed integration step size of 5.0×10^{-5} ps. Conservation of energy to six significant figures is generally obtained. For HONO, the internal dynamics are followed for 82 ps using a step size of 1.5×10^{-4} ps. In this case, energy conservation was generally three significant digits or better.

Initial-state selection for acetylene is accomplished by inserting the zero-point vibrational energy (ZPE) computed from the potential field into each of the normal modes with the molecules in their equilibrium configurations. Subsequently, the equations of motions are integrated for a random period of time after which a selected amount of additional energy is inserted into the local C–H stretching mode in the form of kinetic energy. For HONO, the ZPE of each normal mode is partitioned between kinetic and potential energy with appropriate averaging over the phases of the normal coordinates, followed by selective excitation of the O–H stretch local mode. The coordinates and momenta are then scaled to the desired total energy. The details of this procedure have been fully described elsewhere.[7]

Ensemble spectra are computed by averaging the Fourier transforms of each of 40 trajectories that differ only in the random period or phase averaging used in the initial-state selection.

Molecules containing four atoms, such as HONO and C_2H_2, have six vibrational modes and 15 mode-to-mode rate coefficients. We therefore expect, in principle, a FTIVR spectrum containing as many as 15 energy-transfer peaks plus higher frequency bands resulting from energy transfer to and from the coupling terms along with overtone and combination bands. The assignment of these spectral features to particular mode-to-mode energy-transfer processes is generally a difficult problem. We have found two techniques, heavy-atom blocking and constrained motion, to be particular useful methods to unravel the FTIVR spectrum.

Heavy-atom blocking is a technique originally developed by Rabinovitch *et al.* in their energy flow experiments on cyclic, organometallic compounds.[8] In these experiments, it was found that if two carbon rings are separated by a heavy metal atom, energy flow between the rings is severely restricted. The results obtained with the two-mode, collinear model serve as a simple example of the effect. The same principle may be employed effectively to obtain the band assignments in the FTIVR spectrum. For example, in the acetylene molecule, H–$_1$C–$_2$C–H, if the normal mass of $_1$C, 12 amu, is replaced by a heavy mass of 100 amu, the energy pathway from the H–$_1$C bond to the $_2$C–H stretch motion is effectively blocked. As a result, the spectral bands associated with the blocked energy-transfer pathway(s) will be either missing or significantly reduced in intensity. A comparison of the FTIVR spectra obtained with and without heavy-atom blocking will therefore permit the missing or intensity-reduced peaks to be assigned to the blocked pathways.

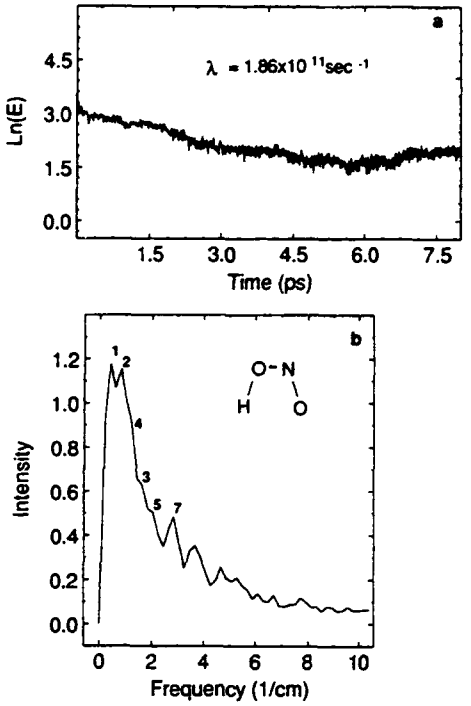

Figure 8. (a) Ensemble average decay curve for the O–H local-mode energy in HONO. The plot is the ensemble average of 40 trajectories. The initial states have ZPE in all of the vibrational modes and sufficient excitation of the O–H local mode to yield a total energy of 2.31 eV. (b) FTIVR spectrum obtained from the average of the Fourier transforms of the local O–H bond energy for each of the trajectories used to obtain the decay plot shown in Figure 1a. The figure inset showing HONO with all atoms written in nonboldface type indicates normal masses are used for all atoms.

The method of constrained motion involves the omission of all initial energy in certain modes of the molecule. This omission serves to significantly reduce or eliminate the coupling between those modes and others in the molecule. As a result, the spectral bands associated with energy transfer between those modes will be reduced in intensity or missing. This intensity change permits the bands assignments to be made. For example, if the initial zero-point torsional mode energy is omitted in HONO, there will be no initial momentum components perpendicular to the molecular plane. In principle, the system will be constrained to planar motion. Consequently, the importance of the torsion pathway in IVR will be substantially reduced, and those spectral bands associated with energy-transfer pathways involving the torsional mode will decrease in intensity.

IV. Results and Discussion

Figure 8a shows the decay of $\log[E_b(t)]$ for HONO at a total energy 2.31 eV, corresponding to zero-point energy in all normal modes with the excess energy initially present as local-mode excitation in the O–H bond. The decay curve is obtained by averaging over the results of 40 trajectories. The general form of the decay curve is as anticipated. There is an approximately

linear decay with several low-frequency oscillations superimposed. Additional higher frequency components are also present.

A total relaxation rate coefficient out of the C–H mode, K_T, can be extracted from these data by fitting the decay curve to a first-order rate law:

$$E_b(t) = E_b(t=0) \exp(-K_T t) \quad (9)$$

so that

$$\log[E_b(t)] = \log[E_b(t=0)] - K_T t \quad (10)$$

By obtaining a linear least-squares fit of eq 10 to the first portion of the data shown in Figure 8a, we obtain $K_T = 1.86 \times 10^{11}$ s^{-1}. Since we expect K_T to be the sum of all of the mode-to-mode rate coefficients out of the local O–H mode, it is clear that the individual mode-to-mode rate coefficients should lie in the range 0.01–0.186 ps^{-1}, where 0.01 ps^{-1} is an assumed lower limit for such coefficients.

The ensemble averages of the Fourier transforms of each of the 40 trajectories yield the results shown in Figure 8b. The energy present in each mode varies as vibrational relaxation proceeds. It is therefore expected that each mode-to-mode coefficient will appear as a broad band covering a range of frequencies that is a reflection of the energy range sampled in the trajectories. This can be seen in the spectra presented in Figures 8–10. Several broad bands are present in the spectral region between 1 and 4 cm^{-1}. The summation of these bands results in six distinct peaks.

The frequencies at which these bands occur represent the average mode-to-mode rate coefficients. The only remaining problem is to determine the modes associated with each peak appearing in Figure 8b. The band assignments are made using heavy-atom blocking and constrained motion methods.

Figure 9a shows the FTIVR spectrum obtained if the masses of the two oxygen atoms and nitrogen in HONO are assigned a value of 100 amu. This assignment will effectively block the energy flow from the O–H stretch to all other modes except the HON bend and out-of-plane torsional mode. The ensemble FTIVR spectrum obtained with this mass combination, using the same random seed, exhibits three peaks, marked as 1, 2, and 3, which appear at the same frequencies as the correspondingly marked bands in Figure 8b. Bands 4, 5, and 7 are missing. Consequently, they must correspond to energy-transfer pathways blocked by the heavy atoms.

Intramolecular vibrational energy redistribution in HONO has been studied extensively by Thompson and co-workers.[7] They have concluded that the major energy-transfer pathway from the O–H stretch is *via* direct transfer to the HON bend followed by transfer from the HON bend to the torsional mode. We therefore assign peak 1, the lowest frequency spectral band in Figures 8b and 9a, to the O–H stretch/torsion. Peak 2, which corresponds to the second fastest energy-transfer rate, is assigned to the HON bend/torsion, and peak 3, the fastest rate, is assigned to the O–H stretch/HON bend.

Figure 9b shows the ensemble FTIVR spectrum obtained when the nitrogen and oxygen atoms in the N–O end group are both assigned masses of 100 amu. We would expect this mass combination to block energy-transfer pathways involving the terminal N–O stretch. As expected, bands 1, 2, and 3 are still present in the spectrum. In addition, three peaks denoted 4, 5, and 6 are also evident. These new peaks are expected to be related to the energy flow paths blocked by the heavy oxygen atom in the H–O–N moiety in Figure 9a. That is, we expect peaks 4, 5, and 6 to involve the O–N stretch and the O–N–O bend.

By employing the constrained motion method, we may obtain the additional information required to make the band assignments. The FTIVR spectrum given in Figure 9c is that obtained when the initial ZPE for the ONO bend is omitted and the terminal N–O atoms are both assigned masses of 100 amu. Comparison

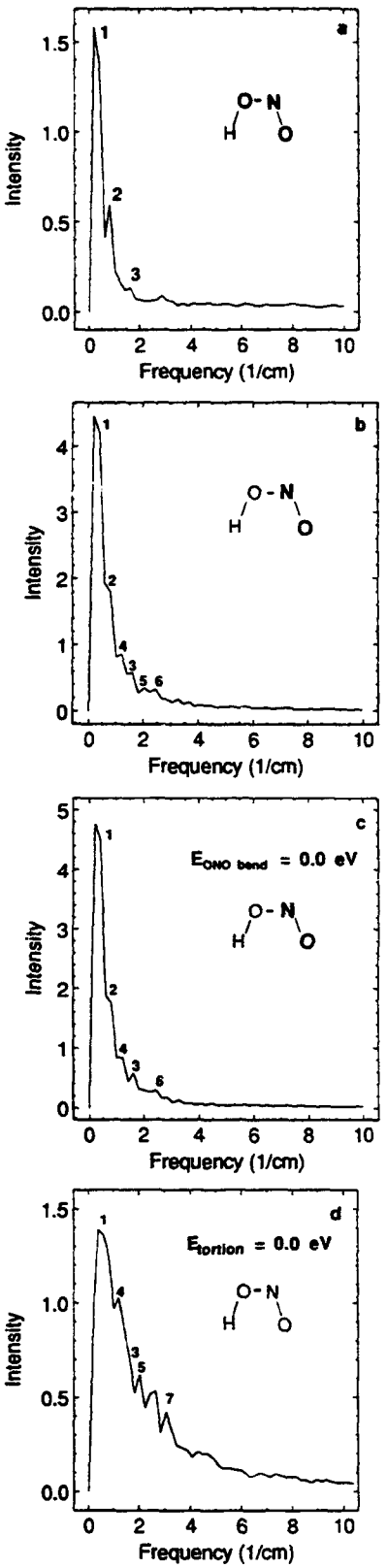

Figure 9. (a) FTIVR spectrum of HONO with ZPE plus sufficient O–H local-mode excitation to yield a total internal energy of 2.31 eV. The atoms in the O–N–O moiety are each assigned a heavy-atom mass of 100 amu. This is denoted by the boldface type in the figure inset. (b) FTIVR spectrum of HONO under the same conditions as in Figure 2a except only the terminal N and O atoms have a heavy mass of 100 amu. Others are normal. (c) FTIVR spectrum of HONO under the same conditions as Figure 2a except the initial ZPE of the ONO bending mode is set to zero. (d) FTIVR spectrum of HONO under same conditions as those given for Figure 8b except the ZPE of the torsional mode is initially set to zero. All masses are normal as indicated by the figure inset.

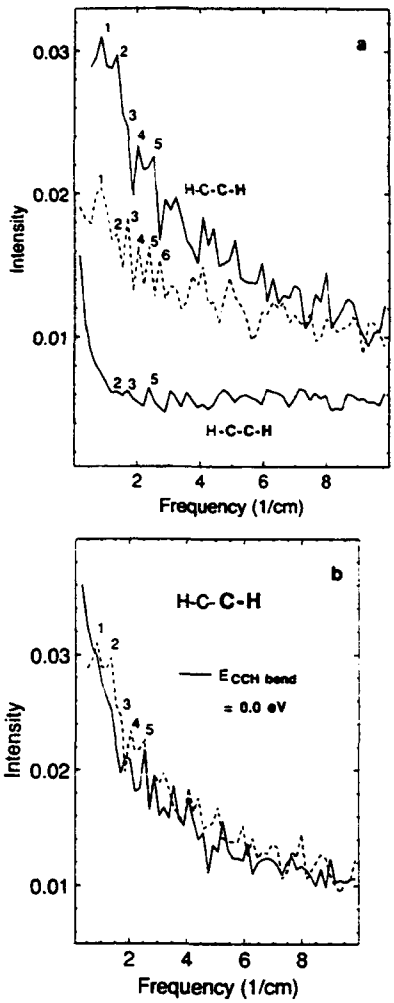

Figure 10. (a) FTIVR spectra for acetylene obtained from the ensemble average of the Fourier transforms of each of 40 trajectories. The initial states have ZPE in all of the vibrational modes and sufficient excitation of the C–H local mode to yield a total energy of 3.18 eV. Dotted spectrum: normal mass for all atoms. Upper solid-line spectrum: terminal (nonexcited) C and H atoms have mass 100 amu. Others have normal mass. Lower solid-line spectrum: atoms in the C–C–H moiety have mass 100 amu. (b) Ensemble average (40 trajectories) FTIVR spectra for acetylene. The dotted spectrum is the same as upper solid-line spectrum shown in (a). The solid-line spectrum is obtained under conditions identical to those for the dotted-line spectrum except the initial ZPE of the CCH bending mode is set to zero.

of parts b and c of Figure 9 shows that peak 5 has disappeared while peaks 4 and 6 remain. We therefore assign band 5 to the O–H stretch/ONO bend energy-transfer pathway.

The remaining assignment is made by noting that peak 6 does not appear in the FTIVR spectrum shown in Figure 8b where all frequencies corresponding to the rates of major energy-transfer paths should be present. We also note that the frequency of peak 6 is exactly double that of peak 4. We therefore take peak 6 to be an overtone of peak 4 and assign the O–H stretch/O–N stretch rate to the frequency of peak 4.

A consistency cross-check may be obtained by setting the initial ZPE of the HONO torsional mode to zero with all atoms assigned their actual mass. Under these conditions, there are no initial momentum components perpendicular to the molecular plane. Therefore, in principle, the system will be constrained to planar motion, and energy-transfer pathways involving the torsional mode will be blocked. [We note that because of numerical integration inaccuracies, some torsional motion may actually occur in the calculations. However, its magnitude should be greatly reduced.] Figure 9d shows the resulting FTIVR ensemble spectrum. Comparison with Figure 8b shows that peak 2 is either absent

TABLE 3: Mode-to-Mode Rate Coefficients for Internal Energy Transfer in C_2H_2 and HONO

molecule	peak no.	transfer path	K (ps^{-1})
C_2H_2	1	C–H stretch/CCH bend	0.026
	2	C–H stretch/torsion	0.041
	3	HCC bend/torsion	0.051
	4	C–H stretch/C–C stretch	0.061
	5	C–H stretch/HCC bend	0.071
	6	C–H stretch/C–H stretch	0.082
HONO	1	O–H stretch/torsion	0.0060
	2	HON bend/torsion	0.024
	3	O–H stretch/HON bend	0.049
	4	O–H stretch/O–N stretch	0.037
	5	O–H stretch/ONO bend	0.061
	7	O–N stretch/N–O stretch	0.085

or significantly reduced in magnitude. This is consistent with our previous assignment of band 2 to the HON bend/torsion pathway. Finally, we note that peak 7 only appears in Figures 8b and 9d, where all atoms have their normal mass. This suggests that this band is associated with the O–N stretch/N–O stretch path. All of the mode-to-mode rate coefficients obtained from the FTIVR spectra for HONO are summarized in Table 3.

A second cross-check on the accuracy of the FTIVR results may be obtained by using them to compute the total relaxation rate of the O–H mode and comparing the value obtained with the IVR relaxation rate computed from eq 10 and the data in Figure 8. Since relaxation of the O–H mode can, in principle, occur by energy transfer to the O–N stretch, the HON bend, the ONO bend, the torsion mode, and N–O stretch, we would expect the total relaxation rate coefficient, K_T, to be given by

$$K_T = K_1 + K_3 + K_4 + K_5 + K_{N-O} \qquad (11)$$

where K_i is the frequency corresponding to peak i. The HONO potential energy surface used in the present study contains no direct coupling terms between the O–H and N–O stretching modes. Consequently, we expect K_{N-O} to be zero for this potential. The fact that we have not been able to identify an FTIVR band corresponding to the O–H stretch/N–O stretch pathway is therefore not surprising. Since K_T is obtained directly from the trajectory results, while the K_i are obtained from the FTIVR band frequencies, the extent to which eq 11 holds constitutes an internal check on the consistency of the results obtained by the two methods.

From Table 3 for HONO, we obtain $(K_1 + K_3 + K_4 + K_5) = 1.53 \times 10^{11}$ s^{-1}. The spectral resolution for each band is 0.20 cm^{-1} or 0.06×10^{11} s^{-1}. We therefore have $(K_1 + K_3 + K_4 + K_5) = (1.53 \pm 0.24) \times 10^{11}$ s^{-1}. The least-squares fitting of eq 10 to the data shown in Figure 8 yields $K_T = 1.86 \times 10^{11}$ s^{-1}. The major uncertainty in this result is related to the arbitrary choice of the initial time period over which the least-squares fitting is performed. By varying this choice within reasonable limits, we estimate that K_T may be varied by about ±10%. Thus, the consistency check compares $(1.53 \pm 0.24) \times 10^{11}$ s^{-1} with $(1.86 \pm 0.19) \times 10^{11}$ s^{-1}. Since the error limits of these values have significant overlap, we conclude that, within the limitations imposed by the spectral resolution and the uncertainty present in the analysis of the trajectory results, the mode-to-mode rate coefficients obtained from the FTIVR spectra and the trajectory-computed overall O–H relaxation rate are consistent.

As an example of a linear molecule, we have applied the FTIVR method to obtain an analysis of intramolecular energy flow in acetylene. The spectra shown in Figure 10a correspond to the ensemble average of the Fourier transform of each of 40 trajectories for acetylene at a total energy of 3.18 eV. This energy comprises zero-point energy in all normal modes with the excess energy initially present as local-mode excitation of one of the H–C bonds. The dotted line shows the FTIVR spectrum for normal C_2H_2 while the solid lines present results for cases involving

heavy-atom blocking. The top line is obtained when the terminal C and H atoms in the C–H bond not initially excited are assigned a mass of 100 amu. Comparison with the dotted line shows that peak 6 is missing while the rest of the bands remain. Peak 6 is therefore assigned to the H–C stretch/C–H stretch pathway.

The bottom solid curve in Figure 10a shows the result when all atoms in the C–C–H moiety are assigned a mass of 100 amu. Under these conditions, we expect only three energy-transfer pathways to be open. the H–C stretch/HCC bend, the H–C stretch/torsion, and the HCC bend/torsion. Comparison with the dotted curve in Figure 10a shows that peaks 1, 4, and 6 have vanished. Only peaks 2, 3, and 5 remain. On the basis of arguments similar to those used for HONO and in the analysis of the FTIVR spectrum for the ethynyl radical,[1] we assign the highest frequency band 5 to the H–C stretch/HCC bend and peak 3 to the HCC bend/torsion. The lower frequency band 2 is interpeted to result from the C–H stretch/torsion pathway.

By elimination and by examination of the predicted rates, band 4 and 1 are assigned to the C–H stretch/C–C stretch and H–C stretch/CCH bend, respectively. The numerous bands at higher frequencies either are associated with energy transfer in and out of the numerous coupling terms in the potential as the model calculations suggest or correspond to overtone or combination bands.

Figure 10b shows the FTIVR spectra for C_2H_2 with two heavy atoms, C and H. The dotted curve is the same as the top solid curve in Figure 10a. The solid curve in Figure 10b is the FTIVR spectrum obtained with the ZPE for the CCH bend and torsional modes initially set to zero. It is seen that bands 1, 2, and 3, which are associated with the H–C stretch/CCH bend, the H–C stretch/torsion, and the HCC bend/torsion, respectively, are considerably reduced as we would expect from the principle of constrained motion. This suggests that the band assignments are correct. The average individual mode-to-mode rate coefficients obtained from the FTIVR spectra for C_2H_2 are summarized in Table 3.

V. Summary and Conclusions

By employing the Fourier transform of a local-mode bond energy, mode-to-mode rate coefficients for classical intramolecular vibrational relaxation have been obtained for HONO and C_2H_2. For both HONO and C_2H_2, six distinct peaks appear in the FTIVR spectrum. The frequencies at which these bands appear are interpreted to correspond to the average mode-to-mode rate coefficients for IVR. To determine the modes associated with each individual peak, heavy-atom blocking and constrained motion methods have been used to close certain energy-transfer paths during vibrational mode relaxation. Comparison of the resulting FTIVR spectra with those obtained under normal conditions permits the accurate assignment of individual bands.

The present results combined with earlier studies on the ethynyl radical[1] show that this FTIVR method works well on three- and four-atom molecules. Previous studies[2] involving an eight-atom molecule, disilane, demonstrate that the method permits the average value of the mode-to-mode rate coefficients to be extracted, but limitation on spectral resolution has, to date, prevented the determination of individual coefficients in such large systems.

Acknowledgment. The authors are indebted to Professor George Schatz for helpful comments related to the implementation of the C_2H_2 potential energy surface. We are pleased to acknowledge financial support from the Air Force Office of Scientific Research (AFOSR) under Grant F49620-92-J-00121 and from the Army Research Office (Grant DAAL03-89-K-0052).

References and Notes

(1) Chang, X. Y.; Thompson, D. L.; Raff, L. M. *Chem. Phys. Lett.* **1993**, *206*, 137.

(2) Schranz, H. W.; Raff, L. M.; Thompson, D. L. *J. Chem. Phys.* **1991**, *95*, 106.

(3) Raff, L. M.; Thompson, D. L. The Classical Trajecotry Approach to Reactive Scattering. In *Theory of Chemical Reaction Dynamics*; Baer, M., Ed.; CRC Press: Boca Raton, FL, Vol. III, p 1.

(4) (a) Qin, Y.; Thompson, D. L. *J. Chem. Phys.* **1992**, *96*, 1992. (b) Guan, Y.; Thompson, D. L. *Chem. Phys.* **1989**, *139*, 147. (c) Guan, Y.; Lynch, G. C.; Thompson, D. L. *J. Chem. Phys.* **1987**, *87*, 6957.

(5) White, K. A.; Schatz, G. C. *J. Phys. Chem.* **1984**, *88*, 2049.

(6) (a) Farantos, S.; Leisegang, E. C.; Murrell, J. N.; Sorbie, K.; Texeria-Dias, J. J. C.; Varandas, A. J. C. *Mol. Phys.* **1977**, *34*, 947. (b) Carter, S.; Mills, I. M.; Murrell, J. N.; Varandas, A. J. C. *Mol. Phys.* **1982**, *45*, 1053.

(7) Thompson, D. L. *Mode Selective Chemistry*; Jortner, J., Ed.; Kluwer Academic Publisher: Dordrecht, 1991 and references therein.

(8) For example, see: (a) Wrigley, S. P.; Rabinovitch, B. S. *Chem. Phys. Lett.* **1983**, *98*, 386. (b) Wrigley, S. P.; Oswald, D. A.; Rabinovitch, B. S. *Chem. Phys. Lett.* **1984**, *104*, 521.